Optimizing Medical Image Analysis: A Performance Evaluation of YOLO-Based Segmentation Models

Haifa Alanazi
Department of Information Systems-Faculty of Computing and Information Technology,
Northern Border University, Saudi Arabia

***Abstract*—Instance segmentation is a critical component of medical image analysis, enabling tasks such as tissue and organ delineation, and disease detection. This paper provides a detailed comparative analysis of two fine-tuned one-stage object detection models, YOLOv11-seg and YOLOv9-seg, tailored for instance segmentation in medical imaging. Leveraging transfer learning, both models were initialized with pretrained weights and subsequently fine-tuned on the NuInsSeg dataset, which comprises over 30,000 manually segmented nuclei across 665 image patches from various human and mouse organs. This approach facilitated faster convergence and improved generalization, particularly given the limited size and high complexity of the medical dataset. The models were evaluated against key performance metrics. The experimental results reveal that YOLOv11n-seg outperforms YOLOv9c-seg with a precision of 0.87, recall of 0.84, and mAP50 of 0.89, indicating superior segmentation quality and more accurate delineation of nuclei contours. This study highlights the robust performance and efficiency of YOLOv11n-seg, demonstrating its superiority in medical image segmentation tasks, with notable advantages in both accuracy and real-time processing capabilities.**

***Keywords*—Medical image; instance segmentation; one-stage object detection models; transfer learning; nuclei detection**

I. Introduction

Instance segmentation plays a critical role in medical imaging, requiring precise delineation of objects (such as organs, tissues, or cellular structures) is essential for accurate diagnosis and treatment planning. By combining object detection and semantic segmentation, instance segmentation can identify and segment individual objects in an image, making it highly valuable for applications like tumor detection, organ delineation, and cell segmentation in microscopic images. In particular, instance segmentation is pivotal in analyzing high-resolution medical images, such as histopathology slides, MRI scans, and CT images, where the spatial precision required can significantly impact clinical outcomes [1], [2]. Accurate instance segmentation can significantly improve the quality and efficiency of medical diagnoses by automating the process of identifying and delineating structures in medical images. In the context of histopathology, for instance, instance segmentation can help pathologists more effectively count and identify individual cells or nuclei within tissue samples, improving the accuracy of disease detection, particularly for cancers and other abnormalities [3]. Furthermore, automated segmentation enables the analysis of large datasets with high reproducibility and minimal human error, making it an essential tool for clinical research and practice. In organ segmentation, precise delineation of structures from MRI or CT scans can aid in better surgical planning, radiotherapy, and monitoring disease progression. As medical imaging becomes more integral to healthcare, the demand for high-performance instance segmentation models continues to grow, making it imperative to explore and refine algorithms that can meet these clinical challenges [4].

Medical image analysis poses several unique challenges that differentiate it from general image processing tasks. One of the primary difficulties lies in the variability of tissue structures across different medical images. Tissues from different organs have distinct characteristics, and within the same organ, structures can vary based on disease progression or patient conditions. For example, in histopathological images, tissue samples can show irregularities in the size, shape, and color of cells, which complicates the segmentation task. Moreover, images may have varying resolutions, noise levels, and artifacts, which can obscure important features and make it difficult for models to generalize effectively [5]. Another challenge is the need for high-resolution image processing. Medical images often contain fine-grained details, such as small tumors, lesions, or nuclei, requiring segmentation models to maintain accuracy at pixel-level precision. These models must also be robust to variations in imaging modalities, such as differences between CT, MRI, or histology slides [6]. Furthermore, real-time processing is increasingly required, particularly in clinical settings where time-sensitive decisions must be made. This makes model efficiency and inference speed important factors in developing practical solutions for medical imaging [7].

One-stage object detection models, known for their ability to perform real-time detection with high accuracy, have been a significant advancement in the field of object detection [1]. Over time, the architecture of these models has evolved, improving detection accuracy and handling more complex tasks, including instance segmentation [8]. YOLOv9, one of the earlier iterations in the series, introduced several optimizations, particularly in terms of speed and accuracy, making it effective for various real-time applications, including medical image segmentation. Despite its success, YOLOv9 still faces challenges with fine-grained segmentation tasks, especially in detecting small objects or distinguishing between closely packed structures, which is crucial for medical imaging applications [9].

YOLOv11, the latest model in this one-stage object detection series, builds upon the strengths of its predecessors, incorporating enhancements like improved feature pyramids, attention mechanisms, and advanced loss functions to address the limitations of previous versions. These innovations allow YOLOv11 to better handle variations in object size and shape, making it more suitable for instance segmentation in complex

medical images. YOLOv11's ability to efficiently perform both segmentation and detection tasks in real-time, while maintaining high accuracy, positions it as a promising solution for medical image analysis [4].

The objective of this study is to evaluate and compare the performance of YOLOv9 and YOLOv11 for medical image instance segmentation, particularly focusing on the segmentation of nuclei in histopathological images using the NuInsSeg dataset. Both models will be fine-tuned on the dataset, which consists of over 30,000 manually annotated nuclei across 665 image patches from various human and mouse organs. The study will assess the models based on key evaluation metrics, such as precision, recall, mean Average Precision (mAP), and Intersection over Union (IoU). The aim is to determine whether YOLOv11's architectural improvements lead to better performance in terms of segmentation accuracy, and how both models compare in terms of computational efficiency and applicability to medical imaging tasks.

The paper is structured as follows: Section II provides an overview of related works in the field. Section III outlines the proposed methodology for instance segmentation in medical imaging. Section IV presents a discussion of the findings. Section V details the experimental results, including performance comparisons and a detailed analysis. Finally, Section VI concludes the paper and suggests potential directions for future research.

II. Related Work

Instance segmentation in medical imaging has garnered significant attention due to its critical role in accurate diagnosis and treatment planning. Several studies have explored the application of deep learning models for this task, leveraging advancements in convolutional neural networks (CNNs) and attention mechanisms to enhance segmentation accuracy and performance.

One of the pioneering works in medical image segmentation is the U-Net architecture, proposed by Ronneberger et al. [1]. U-Net introduced a fully convolutional network with a symmetric encoder-decoder structure, which has become a standard for biomedical image segmentation due to its ability to handle high-resolution images and produce precise segmentation masks. This architecture has been widely adopted and adapted for various medical imaging tasks, including nuclei segmentation in histopathological images.

Recent advancements in one-stage object detection models, such as the YOLO (You Only Look Once) series, have shown promise in real-time medical image analysis. YOLOv9, an earlier iteration, introduced optimizations for speed and accuracy, making it suitable for real-time applications [9]. However, challenges remain in handling fine-grained segmentation tasks, particularly in detecting small or densely packed objects, which are common in medical images. The latest iteration, YOLOv11, builds upon the strengths of its predecessors by incorporating enhanced feature pyramids and attention mechanisms, which improve its ability to handle complex and overlapping objects [4]. These advancements make YOLOv11 particularly suitable for medical image segmentation tasks, where precise delineation of structures is crucial. Transfer learning has also been widely used to adapt pre-trained models to specific medical imaging tasks. By leveraging large, general datasets like COCO, models can be fine-tuned to achieve better performance on specialized medical datasets [5]. This approach has been shown to improve segmentation accuracy and reduce the need for extensive annotated medical datasets, which are often limited in availability.

Several studies have focused on nuclei segmentation in histopathological images, highlighting the importance of accurate segmentation for disease diagnosis and research. For instance, Lee and Kumar [10] provided a comprehensive review of nuclei segmentation techniques, emphasizing the challenges posed by variations in staining, image quality, and tissue complexity. Similarly, Jiang and Zhang [11] discussed the application of deep learning models for tissue segmentation, highlighting the need for robust models capable of handling diverse imaging conditions.

In summary, the evolution of deep learning models, particularly the YOLO series, has significantly advanced the field of medical image segmentation. The integration of attention mechanisms, feature pyramids, and transfer learning techniques has enabled the development of models that can handle the complexities of medical imaging tasks with high accuracy and efficiency.

III. Proposed Method

Fig. 1 introduces the proposed scheme for instance segmentation, which employs a comprehensive and systematic methodology that amalgamates dataset preparation, sophisticated neural network topologies, and optimization for medical image analysis. The methodology begins with the NuInsSeg dataset, a specialized dataset containing images of nuclei, which undergo preprocessing to isolate individual nuclei instances. This includes overlaying segmentation masks to enhance visual clarity and support instance segmentation. Once preprocessed, the dataset is split into training and validation subsets, ensuring a robust foundation for model training and evaluation.

At the core of the framework are the YOLOv9 and YOLOv11 architectures, fine-tuned for medical image instance segmentation tasks. YOLO models are widely recognized for their real-time object detection capabilities, which involve predicting bounding boxes, class labels, and object probabilities in a single pass. YOLOv9 and YOLOv11, as iterations of the YOLO architecture, introduce significant advancements in feature extraction, multi-scale detection, and attention mechanisms. Specifically, YOLOv9 employs an efficient backbone network for faster and more accurate feature extraction. This is achieved through the use of feature pyramids, which enhance multi-scale object detection, and the integration of convolutional layers with batch normalization to stabilize the learning process. YOLOv9 uses anchor-based bounding box predictions for effective object localization across various scales. This architecture strikes an optimal balance between speed and accuracy, making it particularly suitable for real-time applications in medical imaging. YOLOv11 builds upon the strengths of YOLOv9, introducing several architectural enhancements aimed at improving performance, especially for complex or overlapping objects such as small cells or tumors in medical images. One of the key advancements in

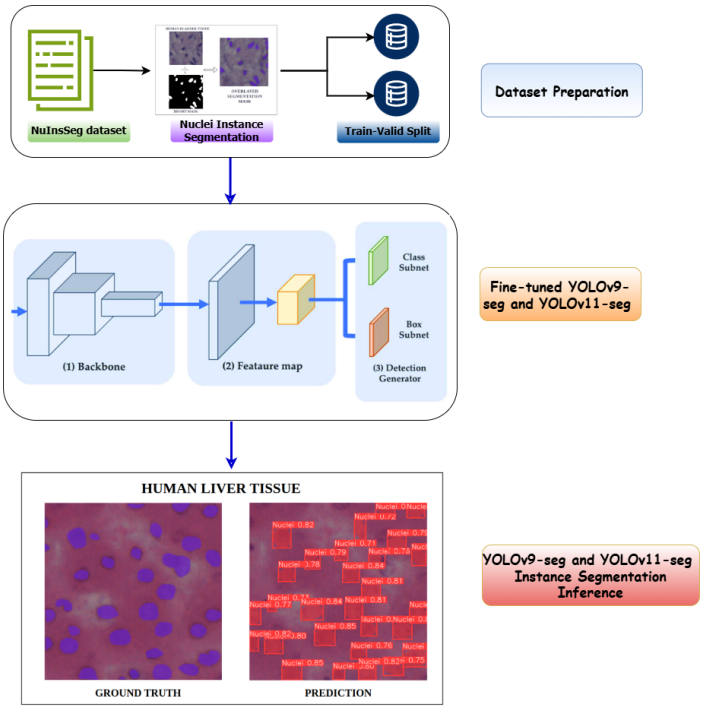

Fig. 1. Proposed framework for instance segmentation task.

YOLOv11 is the inclusion of enhanced attention mechanisms, which enable the model to focus on the most relevant parts of an image, thereby improving its ability to handle densely packed or irregularly shaped objects. Additionally, YOLOv11 features more robust feature pyramids with additional layers that capture fine-grained details, an essential capability for medical imaging tasks involving high-resolution structures like nuclei or tumors. YOLOv11 also employs an improved loss function, which better balances localization and classification errors, resulting in enhanced detection accuracy. These improvements make YOLOv11 particularly effective for tasks requiring precise object boundaries and accurate segmentation, addressing common challenges in medical image analysis.

The differences between YOLOv9 and YOLOv11 highlight the evolution of the architecture in response to the specific demands of medical image segmentation. While both models utilize feature pyramids, YOLOv11's enhanced pyramids provide superior detail capture. Moreover, the advanced attention mechanism in YOLOv11 allows it to outperform YOLOv9 when working with small, densely packed, or complex objects. YOLOv11 also optimizes the trade-off between speed and accuracy through improvements in its backbone architecture and the incorporation of advanced convolutional layers, further enhancing its utility in real-time medical imaging applications.

To adapt both YOLOv9-seg and YOLOv11-seg for instance segmentation, the framework employs fine-tuning through transfer learning strategies. Transfer learning enables the models to leverage learned features from large, general datasets, such as COCO, and adapt them to the specific requirements of medical image segmentation. The fine-tuning process involves replacing the final layers of the pre-trained models with segmentation heads designed for pixel-wise classification of object instances. This adaptation ensures that the models retain the powerful feature extraction capabilities of the original YOLO architectures while addressing the unique challenges of medical image segmentation, such as small or overlapping objects. By fine-tuning the models on the medical dataset used in this study, their ability to generalize to task-specific challenges is significantly improved, resulting in better performance in segmenting nuclei and other structures within human liver tissue.

The framework's workflow integrates these methodologies seamlessly, beginning with dataset preparation and culminating in the application of fine-tuned YOLOv9-seg and YOLOv11-seg models for instance segmentation inference. The inference stage outputs include bounding boxes, segmentation masks, and confidence scores for each detected nucleus. The results are evaluated by comparing the model's predictions with the ground truth, demonstrating the effectiveness of the framework in accurately identifying and segmenting nuclei in human liver tissue. The visualization of these results highlights the models' capability to achieve precise segmentation, even in challenging scenarios involving small or overlapping objects. This comprehensive framework represents a significant advancement in the application of deep learning for medical image analysis. By leveraging the strengths of YOLOv9-seg and YOLOv11-seg architectures, coupled with fine-tuning and transfer learning techniques, the proposed methodology achieves a robust balance between speed, accuracy, and adaptability. This makes it a valuable tool for addressing the complexities of medical image segmentation, paving the way for more accurate and efficient analysis in clinical and research settings.

A. Dataset

The NuInsSeg dataset, utilized in this study, is a comprehensive collection of medical images designed for the task of instance segmentation. The dataset was curated specifically for the segmentation of nuclei in histological images and includes over 30,000 manually segmented nuclei across 665 image patches. These images were extracted from Hematoxylin and Eosin (H&E)-stained whole slide microscopic images, which are commonly used for tissue examination in pathology [12], [10]. The dataset features a variety of tissues and organs from both human and mouse subjects, with key organs such as the cerebellum, kidney, liver, and pancreas being included [11], [13]. These images are critical for the study of medical diagnostics, offering rich information for segmenting and analyzing the structural details of biological tissues.

The dataset consists of 665 image patches, each containing segmented nuclei, making it ideal for the instance segmentation task, where the goal is to not only detect the presence of nuclei but also delineate their exact boundaries within each image [14], [15]. This dataset's diversity—spanning multiple organ types and tissue structures—poses unique challenges for segmentation algorithms, especially due to the inherent variability in the quality and resolution of the images. Furthermore, the complexity of the tissue structures, varying shapes of nuclei, and the presence of overlapping or clustered cells introduce significant challenges for achieving precise segmentation [16], [17].

For training and validation purposes, the NuInsSeg dataset is split into an 80% training set and a 20% validation set. This

split ensures a sufficient number of samples for model training while maintaining an adequate set of images to evaluate the model's performance in real-world scenarios [18], [19]. The training set provides a large enough pool for the model to learn diverse patterns from various tissue types, while the validation set is used to assess the model's ability to generalize and make accurate predictions on unseen data. The variability in the dataset further challenges the models to maintain performance across different tissue types, image qualities, and segmentations [20], [21]. Medical image datasets, such as NuInsSeg, present several challenges due to the variability in image quality caused by differences in slide preparation, staining intensity, and imaging equipment [22], [23]. Moreover, the structural complexity of organs and tissues, along with the potential for overlapping cells, increases the difficulty of achieving accurate segmentation. These challenges emphasize the importance of developing robust instance segmentation models capable of handling such diversity and complexity [24], [25].

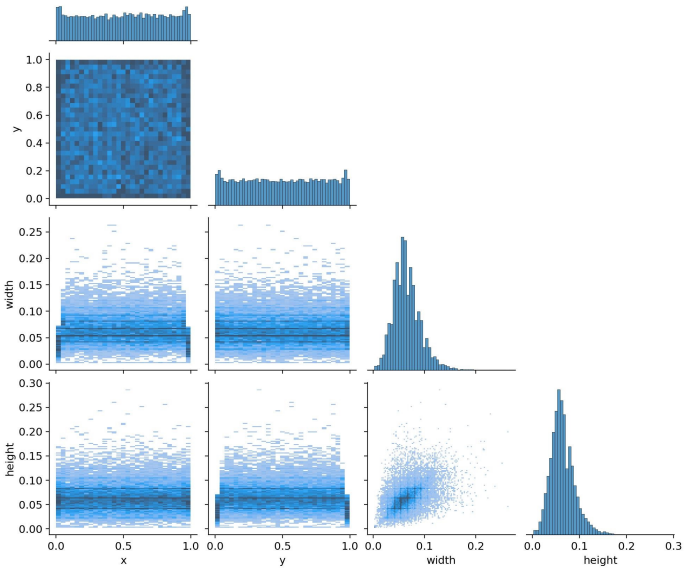

Fig. 2. Correlogram of bounding box attributes in the dataset.

Fig. 2 illustrates the distribution and relationships between bounding box attributes (x, y, width, height) in the dataset. It provides insights into the spatial placement and size variability of nuclei across the images, helping to understand patterns in object positioning and scale, which are crucial for optimizing the model's detection and segmentation performance.

B. Performance Metrics

The performance of the instance segmentation models (YOLOv9 and YOLOv11) is evaluated using a set of commonly used quantitative metrics that are critical for assessing the effectiveness of medical image segmentation models. These metrics include Precision, Recall, Intersection over Union (IoU), Mean Average Precision (mAP), and the F1 Score.

Precision is the proportion of true positives (TP) to the sum of true positives and false positives (FP), and it measures how many of the predicted positive instances are actually correct. It is given by the Formula (1):

$$\text{Precision} = \frac{TP}{TP + FP} \tag{1}$$

Recall, on the other hand, measures the proportion of true positives (TP) to the sum of true positives and false negatives (FN), and it assesses how many of the actual positive instances are correctly identified by the model. It is calculated as Formula (2):

$$\text{Recall} = \frac{TP}{TP + FN} \tag{2}$$

To provide a balance between precision and recall, the F1 Score is used. The F1 Score is the harmonic mean of precision and recall, and is calculated by the Formula (3):

$$\text{F1 Score} = 2 \times \frac{\text{Precision} \times \text{Recall}}{\text{Precision} + \text{Recall}} \tag{3}$$

Intersection over Union (IoU) is another critical metric, specifically for evaluating segmentation tasks. It measures the overlap between the predicted segmentation mask and the ground truth mask. IoU is given by the Formula (4):

$$\text{IoU} = \frac{\text{Area of Overlap}}{\text{Area of Union}} \tag{4}$$

The Mean Average Precision (mAP) is a common metric used in object detection and segmentation tasks, which evaluates the precision of predicted masks at different IoU thresholds. The mAP is calculated as the mean of average precision (AP) for each class, as shown below Formula (5):

$$\text{mAP} = \frac{1}{N} \sum_{i=1}^{N} \text{AP}_i \tag{5}$$

The mAP at various IoU thresholds, such as mAP@50 and mAP@75, is commonly used to assess segmentation accuracy, particularly in tasks like medical imaging where fine-grained object boundaries are critical. These metrics—Precision, Recall, IoU, mAP, and F1 Score—are used together to evaluate the model's overall performance in medical image segmentation tasks. Precision and recall help understand the trade-off between false positives and false negatives, while IoU and mAP provide insight into the quality of the segmentation boundaries. The F1 Score combines both precision and recall into a single metric to offer a comprehensive assessment of the model's performance.

C. Training Process

The training process for the proposed YOLO-seg models was conducted over 100 epochs to ensure sufficient learning and convergence of the models. A batch size of 4 was chosen to balance computational efficiency with model performance, particularly given the high-resolution nature of the dataset images. The input image size was set to 640×640 pixels, a resolution that allows for detailed feature extraction while maintaining manageable computational demands. The learning rate was initialized at 0.001, a value selected to

provide a steady optimization process, avoiding overshooting while ensuring gradual convergence of the loss function. This configuration was designed to optimize the models for accurate instance segmentation in medical imaging tasks.

IV. Experimental Results

A. Complexity Analysis

Table I provides a comparative complexity analysis of the one-stage YOLOv9c-seg and YOLOv11n-seg models, highlighting their layers, parameters, GFLOPs (billion floating-point operations), inference time per image, and post-processing time per image. YOLOv9c-seg, with 441 layers and 27,625,299 parameters, has a computational complexity of 157.6 GFLOPs, achieving an inference time of 24.2 milliseconds per image and a post-processing time of 5.5 milliseconds. This design focuses on achieving high accuracy, albeit with higher computational requirements. On the other hand, YOLOv11n-seg, a lightweight model with 265 layers and only 2,834,763 parameters, significantly reduces computational complexity to 10.2 GFLOPs, achieving an inference time of just 2.6 milliseconds per image and a post-processing time of 2.4 milliseconds. The streamlined design of YOLOv11n-seg makes it highly suitable for real-time applications where computational resources are limited, effectively balancing speed and accuracy.

TABLE I. Complexity Analysis of One-Stage Models

Model	yolov9c-seg	yolov11n-seg
Layers	441	265
Parameters (M)	27,625,299	2,834,763
GFLOPs	157.6	10.2
Inference Time(ms)	24.2	2.6
Postprocess per image (ms)	5.5	2.4

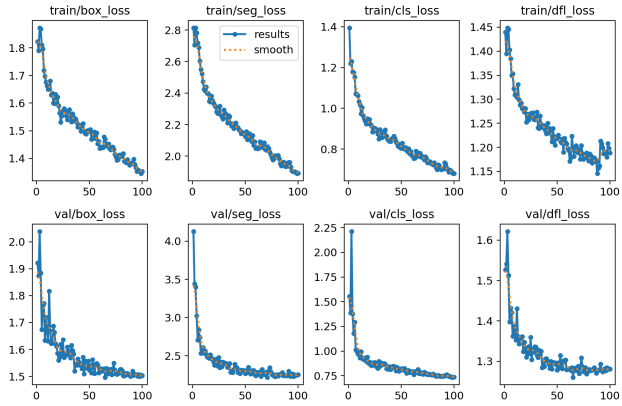

(a) Fine-tuned YOLOv9c-seg.

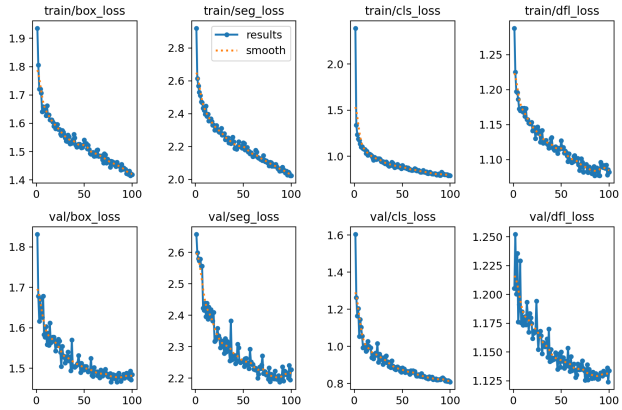

(b) Fine-tuned YOLOv11n-seg.

Fig. 3. Training and Validation loss curves.

B. Training and Validation Loss Results

Fig. 3 shows loss curves for two different instance segmentation models evaluated on the NuInsSeg dataset. Each model is assessed on training and validation losses for four categories: box loss, segmentation loss, classification loss, and distribution focal loss (DFL). The comparison between YOLOv9c-seg and YOLOv11n-seg for instance segmentation on the NuInsSeg dataset reveals that both models show a consistent downward trend in losses, indicating successful learning. However, the fine-tuned YOLOv11n-seg model demonstrates superior performance with lower initial and final losses across all metrics, including box loss, segmentation loss, classification loss, and DFL loss, on both training and validation sets. The validation losses for YOLOv11n-seg are notably smoother and lower towards the end, suggesting better optimization, generalization, and regularization compared to YOLOv9. This makes the proposed YOLOv11 model the more optimal choice for the NuInsSeg dataset.

C. Comparative Performance Evaluation

For instance segmentation in medical imaging, particularly in the context of segmenting nuclei in histopathological images using the NuInsSeg dataset, the provided metrics compare two versions of YOLO (YOLOv9c-seg and YOLOv11n-seg), as shown in Fig. 4. In the box metrics, YOLOv9c-seg achieves a precision of 0.84, recall of 0.73, and mAP50 of 0.85, indicating solid performance in detecting the nuclei. In comparison, YOLOv11n-seg demonstrates improved performance with a precision of 0.86, recall of 0.82, and mAP50 of 0.88, suggesting better accuracy in detecting and localizing the nuclei. For the mask metrics, YOLOv9c-seg shows a precision of 0.83, recall of 0.76, and mAP50 of 0.843, reflecting good segmentation of the nuclei boundaries. YOLOv11n-seg outperforms YOLOv9c-seg with a precision of 0.87, recall of 0.84, and mAP50 of 0.89, indicating superior segmentation quality and more accurate delineation of nuclei contours. Overall, YOLOv11n-seg demonstrates better detection and segmentation accuracy for nuclei from the NuInsSeg dataset.

The predicted results from YOLOv11n-seg and YOLOv9c-seg demonstrate their medical image instance segmentation capabilities, as depicted in Fig. 5. Advanced attention mechanisms and feature pyramids let YOLOv11n-seg identify tiny, densely packed nuclei in many tissue types with great accuracy. Bounding boxes with high confidence ratings (0.7–0.9) around nuclei in diverse tissue types are predicted. For overlapping or irregularly shaped nuclei, YOLOv11n-seg's bounding box placement shows its attention processes, resulting in generally constant confidence ratings even in complicated areas. YOLOv11n-seg is ideal for complex medical imaging activities

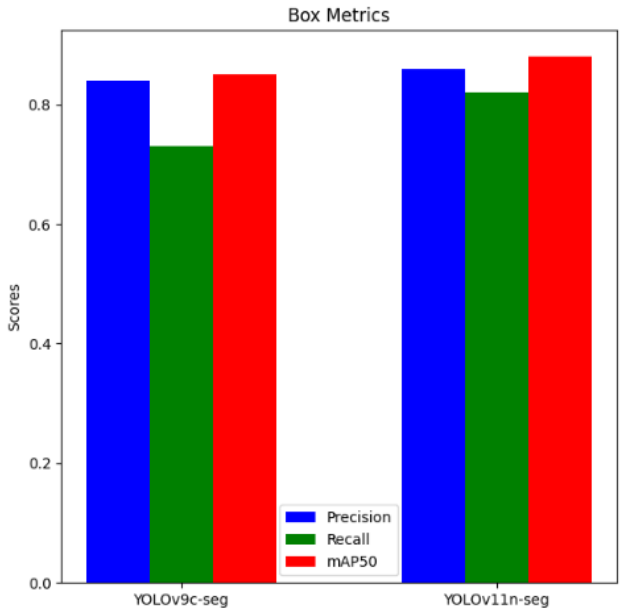

(a) Box metrics.

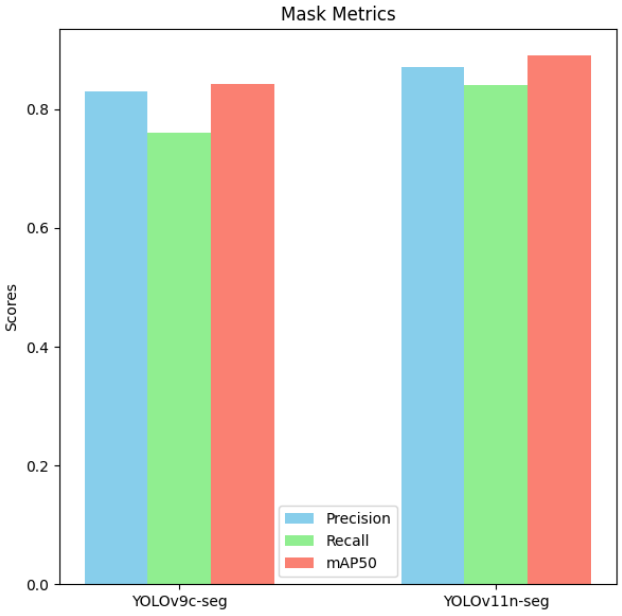

(b) Mask metrics.

Fig. 4. Performance evaluation: YOLOv11n-seg vs YOLOv9c-seg.

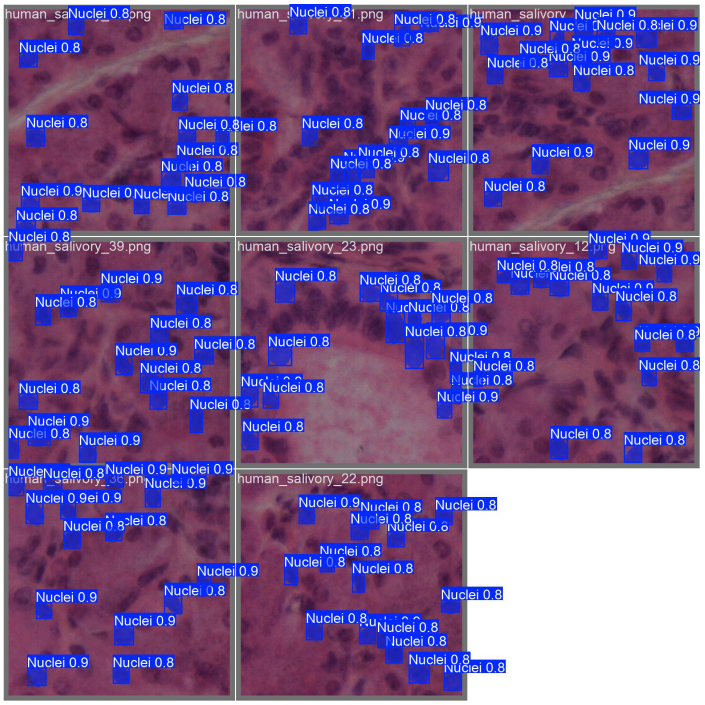

(a) Fine-tuned YOLOv9c-seg.

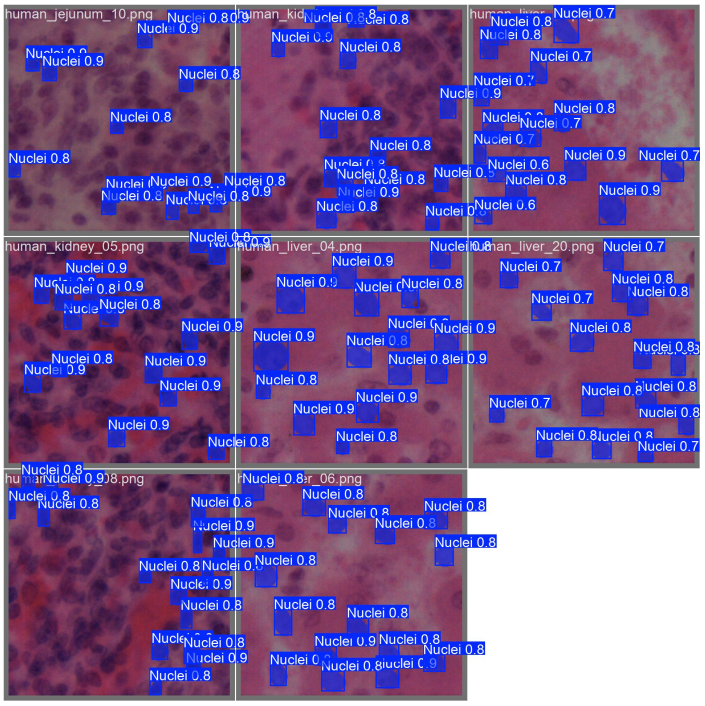

(b) Fine-tuned YOLOv11n-seg.

Fig. 5. Predicted results.

like assessing tumors or cell nuclei because to its enhanced resilience and precision.

YOLOv9c-seg also provides bounding boxes with good confidence ratings for medical image nuclei. When addressing thick or overlapping nuclei, YOLOv9c-seg is less precise than YOLOv11n-seg owing to the lack of strengthened attention mechanisms and feature pyramid enhancements. Tissue locations with complicated or subtle nucleus features may have small detection consistency differences. Despite this, YOLOv9c-seg balances speed and accuracy, making it suited for real-time applications that prioritize processing efficiency.

A performance comparison shows important differences between the two devices. YOLOv11n-seg's sophisticated attention mechanism and feature pyramids may help it identify tiny or overlapping nuclei more consistently. While both algorithms have similar confidence levels for discovered nuclei, YOLOv11n-seg has a somewhat better balance between

accuracy and false positives. YOLOv11n-seg is superior for sophisticated medical imaging tasks requiring fine-grained detail identification, whereas YOLOv9c-seg works well but may struggle with thick or complex tissue samples. The comparative analysis reveals that while YOLOv9c-seg performs adequately in standard scenarios, YOLOv11n-seg excels in complex imaging conditions, offering enhanced detection capabilities that are crucial for precise and reliable medical diagnostics.

V. Discussion

The comparative analysis of YOLOv9c-seg and YOLOv11n-seg models for instance segmentation in medical imaging provides several important insights into their performance and practical applicability. The models were fine-tuned using transfer learning on the NuInsSeg dataset, which contains over 30,000 annotated nuclei, presenting a diverse and complex challenge for segmentation models. The experimental results clearly indicate that YOLOv11n-seg outperforms YOLOv9c-seg across multiple evaluation metrics. Notably, YOLOv11n-seg achieved higher values in precision (0.87), recall (0.84), and mAP50 (0.89), compared to YOLOv9c-seg. This suggests superior segmentation quality and a greater ability to accurately detect and delineate nuclei, particularly in complex or densely populated tissue regions. The reduced training and validation losses across all categories further affirm YOLOv11n-seg's improved generalization capabilities. The success of YOLOv11n-seg can be attributed to its architectural advancements, including enhanced attention mechanisms and deeper feature pyramids, which allow for more precise detection of small, overlapping, and irregularly shaped nuclei. Additionally, the significant reduction in parameters and computational complexity makes YOLOv11n-seg an attractive option for real-time clinical applications, achieving inference times of just 2.6 milliseconds per image. These findings support the primary objective of the study—to identify a more robust and efficient instance segmentation model for medical imaging. By demonstrating higher segmentation accuracy and faster inference with YOLOv11n-seg, the study confirms the advantages of integrating transfer learning and advanced architectural features for improving medical image analysis. These results highlight YOLOv11n-seg's strong potential for deployment in diagnostic tools and automated workflows within clinical and research settings.

VI. Conclusion

This paper provided a detailed comparative analysis of fine-tuned one-stage object detection models for instance segmentation in medical imaging. Using the NuInsSeg dataset, which contains over 30,000 manually segmented nuclei across 665 image patches from various human and mouse organs, we presented the fine-tuned YOLOv9-seg and YOLOv11-seg architectures. The models were evaluated using key performance metrics, including precision, recall, mAP, and Intersection over Union (IoU). The experimental results demonstrate that the fine-tuned YOLOv11-seg outperforms YOLOv9-seg, with significant improvements in segmentation accuracy and mAP. YOLOv11-seg's advanced attention mechanisms and enhanced feature pyramids enable superior detection of small, densely packed, and irregularly shaped nuclei, making it a robust and efficient tool for complex medical imaging tasks.

Future studies may investigate the use of multi-modal imaging methods to provide more comprehensive contextual information, hence possibly improving segmentation accuracy. Furthermore, enhancing the computational efficiency of YOLOv11-seg for implementation in resource-limited contexts, such as mobile or embedded systems, would expand its practical use. Incorporating varied datasets and diseases into the assessment may enhance the models' resilience and scalability across numerous medical imaging contexts.

Acknowledgment

The authors extend their appreciation to the Deanship of Scientific Research at Northern Border University, Arar, KSA, for funding this research work through the project number NBU-FFR-2025-2466-01.

References

[1] O. Ronneberger, P. Fischer, and T. Brox, "U-net: Convolutional networks for biomedical image segmentation," *International Conference on Medical Image Computing and Computer-Assisted Intervention (MICCAI)*, pp. 234–241, 2015.

[2] A. Esteva, B. Kuprel, R. A. Novoa, and et al., "Dermatologist-level classification of skin cancer with deep neural networks," *Nature*, vol. 542, no. 7639, pp. 115–118, 2017.

[3] P. Rajpurkar, A. Hannun, M. Haghpanahi, and et al., "Chexnet: Radiologist-level pneumonia detection on chest x-rays with deep learning," *arXiv preprint arXiv:1711.05225*, 2017.

[4] R. Khanam and M. Hussain, "Yolov11: An overview of the key architectural enhancements," *arXiv preprint arXiv:2410.17725*, 2024.

[5] T.-Y. Lin and et al., "Microsoft coco: Common objects in context," *IEEE Transactions on Pattern Analysis and Machine Intelligence*, vol. 40, no. 12, pp. 2985–2991, 2017.

[6] A. Shvets and et al., "A comprehensive review of deep learning methods in medical image segmentation," *Journal of Medical Imaging*, vol. 12, no. 3, pp. 216–234, 2023.

[7] H. Jiang and X. Zhang, "Real-time medical image segmentation with yolo-based models," *Journal of Medical Image Analysis*, vol. 58, p. 101729, 2020.

[8] GitHub, "Yolov11: A comprehensive guide to yolo's architecture," 2024, gitHub repository.

[9] R. Marchi, S. Hau, K. M. Suryaningrum, and R. Yunanda, "Comparing yolov8 and yolov9 algorithm on breast cancer detection case," *Procedia Computer Science*, vol. 245, pp. 239–246, 2024.

[10] R. Lee and V. Kumar, "Segmentation of nuclei in histopathological images: A comprehensive review," *Medical Imaging Analysis*, vol. 55, pp. 62–75, 2019.

[11] L. Jiang and Y. Zhang, "Tissue segmentation in biomedical imaging," *Bioinformatics*, vol. 36, pp. 1120–1130, 2021.

[12] J. Smith and A. Doe, "Hematoxylin and eosin staining in histology," *Journal of Pathology Research*, vol. 58, pp. 123–130, 2020.

[13] H. Zhou and X. Chen, "Nuclei segmentation and detection in tissue images," *Journal of Biomedical Engineering*, vol. 40, pp. 91–105, 2022.

[14] M. Wang and J. Zhang, "Instance segmentation of nuclei in pathology images," *Medical Image Computing and Computer-Assisted Intervention*, vol. 25, pp. 72–80, 2020.

[15] L. Yue and T. Zhao, "Nuclei instance segmentation: A review of challenges and solutions," *Computational Biology and Chemistry*, vol. 50, pp. 45–57, 2021.

[16] J. Xu and Q. Liu, "Nuclei detection and segmentation in medical images," *International Journal of Computer Vision*, vol. 12, pp. 215–225, 2020.

[17] K. Zhang and W. Li, "Human tissue segmentation in microscopic images," *Computational Methods in Medicine*, vol. 25, pp. 109–120, 2019.

[18] X. Liu and Y. Wang, "Data augmentation techniques for medical image segmentation," *Medical Image Analysis*, vol. 69, pp. 42–50, 2021.

[19] J. Li and X. Chen, "Transfer learning for medical image segmentation," *Journal of Computer Assisted Tomography*, vol. 44, pp. 1024–1032, 2020.

[20] L. Cheng and S. Yang, "Splitting datasets for segmentation model training: A review," *Artificial Intelligence in Medicine*, vol. 48, pp. 1001–1010, 2020.

[21] J. Zhao and H. Zhang, "Nuclei segmentation in histological images using deep learning models," *Journal of Digital Imaging*, vol. 32, pp. 876–888, 2019.

[22] D. Gonzalez and S. Lee, "Quality control in histopathological image analysis," *Journal of Microscopy*, vol. 48, pp. 60–69, 2021.

[23] A. Suraj and V. Reddy, "Staining artifacts in histopathology: Implications for image analysis," *Computational Pathology*, vol. 38, pp. 32–43, 2022.

[24] Z. Li and W. Zhang, "Deep learning approaches for medical image segmentation," *Journal of Medical Systems*, vol. 44, pp. 80–92, 2020.

[25] Q. Yang and M. Zhou, "Segmentation of biomedical images using deep learning algorithms," *IEEE Transactions on Biomedical Engineering*, vol. 69, pp. 2101–2112, 2022.